

Quality, Compatibility and Synergy Analyses of Global Aerosol Products

*M.-J. Jeong and Z. Li
Department of Meteorology
University of Maryland
College Park, Maryland*

*D. A. Chu and S.-C. Tsay
Laboratory for Atmospheres
NASA Goddard Space Flight Center
Greenbelt, Maryland*

Introduction

Global aerosol products play an important role in climate change studies due to their complex direct and indirect effects. While numerous global aerosol products have been generated from various satellite sensors, much more insight into these products is needed to understand them in terms of their strengths, weaknesses and synergies, in order to 1) make informative and creative use of the data, 2) to extract as much information as possible from the data, and 3) to filter out any inherent noise and uncertainties for future improvement in both data quality and quantity. Presented here is a preliminary study towards achieving this goal by examining the quality, compatibility and synergy among four prominent global aerosol products derived from advanced very high resolution radiometer (AVHRR), total ozone mapping experiment spectrometer (TOMS), and moderate-resolution imaging spectroradiometer (MODIS) (Mishchenko et al. 1999, Torres et al. 2002, Herman et al. 1997, Tanré et al. 1997).

Regional Analysis using the AVHRR and TOMS Aerosol Products

The following regions were selected based on certain unique features that have not been previously addressed: off the coast of Peru, a tropical zone between western Africa to Eastern Central Pacific, and North Pacific regions. First, the high aerosol optical thickness (AOT) associated with small **airborne emission?** (AE) off the shores of Peru is due to cloud contamination. If this were not so, the presence of small AE would contradict other studies that reported small particles in this region and argued about the apparent evidence of an aerosol indirect effect. Second, the long plumes of enhanced AOT along the Equatorial Eastern Pacific (EC Pacific) have a complex and interesting seasonality that is driven by atmospheric circulation. The plume is a manifestation of the convergence of various types of aerosols (dust, smoke, pollution aerosols, etc.) transported by prevailing winds that change with season. Third, the generally enhanced aerosol field over the North Pacific is found to consist primarily of fine-mode aerosols and the loading responds sharply to the changes in wind direction, signifying heavy influence by aerosols (especially pollution) transported from Asia. However, there is no discernible dust signal in terms of relative values of AE even during the dust-active season in spring. This could be due to the

smearing out of sporadic dust episodes by averaging in a month or due to the misclassification of dust as cloud. On the other hand, significant correlations found between the AVHRR AOT and chlorophyll concentration around these regions suggest a possible influence of ocean color contamination and/or induced oceanic aerosols such as nss-sulfate, which can be linked to phytoplankton activity.

Compatibility and Synergy between the AVHRR and TOMS Aerosol Products

The AVHRR and TOMS aerosol products also exhibit a good synergy, which is exploited here. For example, TOMS data alone has difficulty in differentiating between dust and biomass burning aerosols, which can be compensated for by the AVHRR AE pertaining to aerosol size. Taking advantage of their respective strengths, we developed an algorithm to classify aerosol types into dust, biomass burning, a mixture of the two, sulfate/pollution, and sea-salt, etc. Using this algorithm, regions under the dominant influence of various types of aerosols are determined from the two satellite products alone (Figure 1).

Prior to MODIS and multi-angle imaging spectrometer (MISR), it has been difficult to gain such information from a single satellite. The performance of this algorithm is influenced by the quality of each aerosol product (especially the AVHRR AE and the TOMS aerosol index [AI]).

As an application of the classification and exploitation of the synergy, the two AOT products are integrated to generate an AOT product at a common wavelength (0.55 μm) of truly global coverage covering both ocean and land (Figure 2). To reduce the large scattering and biases exhibited when direct comparisons of the two products were made, different relationships were derived between the TOMS and AVHRR AOTs according to aerosol type (Figure 3). The range of uncertainty of the estimated AOT is $\pm 0.08 \pm 0.20 \tau$. These inferred AOTs are compared to AERONET measurements, and most of the estimations fall within this range of uncertainty (Figure 4).

Compatibility between the AVHRR and the MODIS Aerosol Products

In light of large discrepancies among various satellite-based global aerosol products, two prominent monthly global aerosol products retrieved from AVHRR (Mishchenko et al. 1999) and MODIS (Tanré et al. 1997) measurements are compared and factors leading to their discrepancies are explored. Comparisons of the monthly aerosol optical thickness (AOT) at 1 x 1 degree resolution showed substantial scattering and moderate systematic differences. However, their regional means (also long-term means) are much better correlated with the general tendency that the AVHRR values are smaller than the MODIS values, especially for heavy aerosol loadings (Figure 5). The difference in cloud screening is likely a factor (Myhre et al. 2004), but other factors can also come into play, for example, use of different aerosol models differentiated in size distribution function and refractive index.

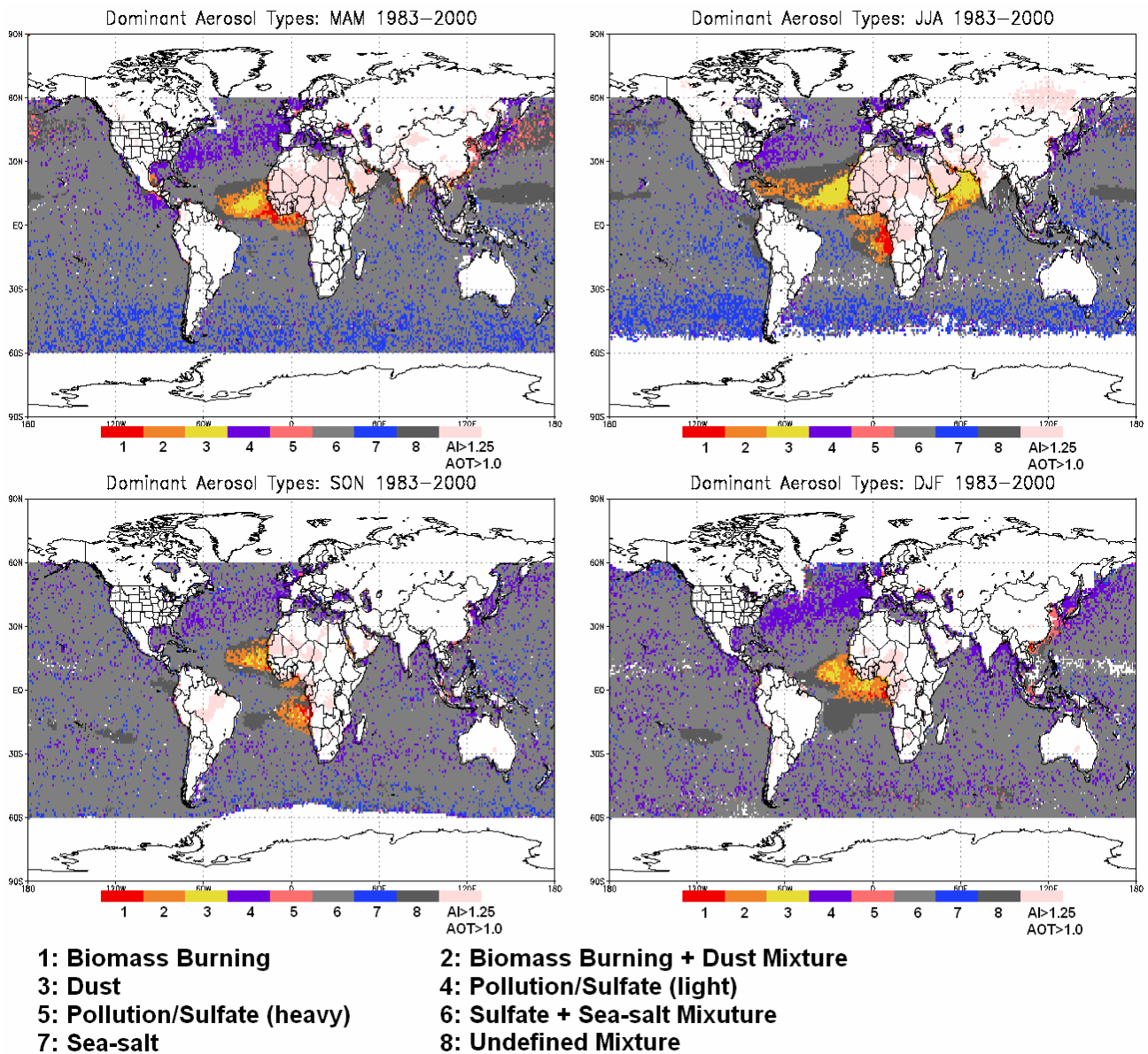


Figure 1. Global seasonal maps of dominant aerosol types based on a classification algorithm for identification of dominant type(s) of aerosols. Land areas with TOMS AOT greater than 1 and AI greater than 1.25 are colored in light pink to indicate major aerosol sources.

The MODIS retrieval algorithm employs 20 combinations of aerosol size distributions given by bi-log-normal (BL) functions with variable refractive index. The AVHRR algorithm used a modified power (MP) law size distribution with a fixed refractive index. Extensive model simulations were conducted to investigate the impact of the differences in the size distribution function and the refractive index on the AOT discrepancies (Figure 6). It is found that the difference in the size distribution function can bring about substantial AOT discrepancies of up to a factor of 2, while different refractive indices cause a moderate systematic difference. The discrepancies depend on the similarity in aerosol size modes

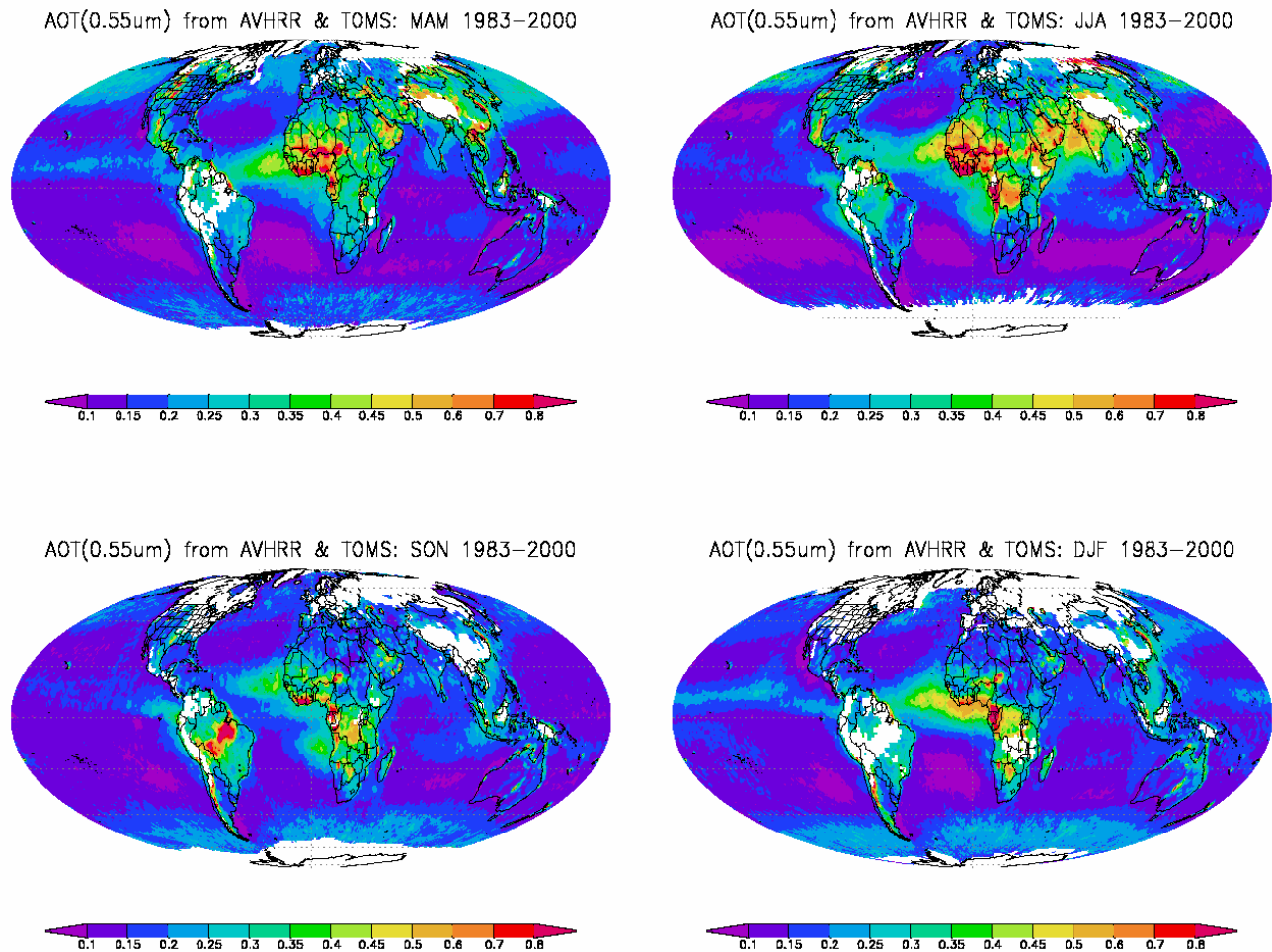


Figure 2. Global maps of seasonal mean AOT at $0.55\mu\text{m}$. AOT over land was estimated from regression equations based on relationships among TOMS AOT and AI and AVHRR AOT. AOT over the ocean is the AVHRR AOT as originally reported.

selected by the two algorithms. More drastic underestimations of AOT by the AVHRR relative to the MODIS is more likely induced by the differences in cloud screening including misclassification of heavy aerosols as clouds in the AVHRR product. Thus, more attention should be paid to aerosol size distributions in addition to refractive index and cloud screening.

Larger discrepancies exist in the Ångström exponent (α) derived from the MODIS and the AVHRR. The AVHRR retrievals seem to suffer from random-like errors with low signal-to-noise ratio. In comparison, the MODIS α product is of better quality in terms of spatial variation and its correlation with the AOT (Figure 7). We attempted to understand the discrepancies between α derived from the MODIS and the AVHRR by simulating the effects of aerosol size distribution function and refractive indices on α retrieval. Our model simulations also point to a big contribution by different aerosol models used in the AVHRR and MODIS retrieval algorithms. The influence of aerosol size distribution on the estimation of aerosol effective radius from α is also evaluated. For a given α , the corresponding aerosol effective radii may differ by more than $1\mu\text{m}$ among the various size distribution functions.

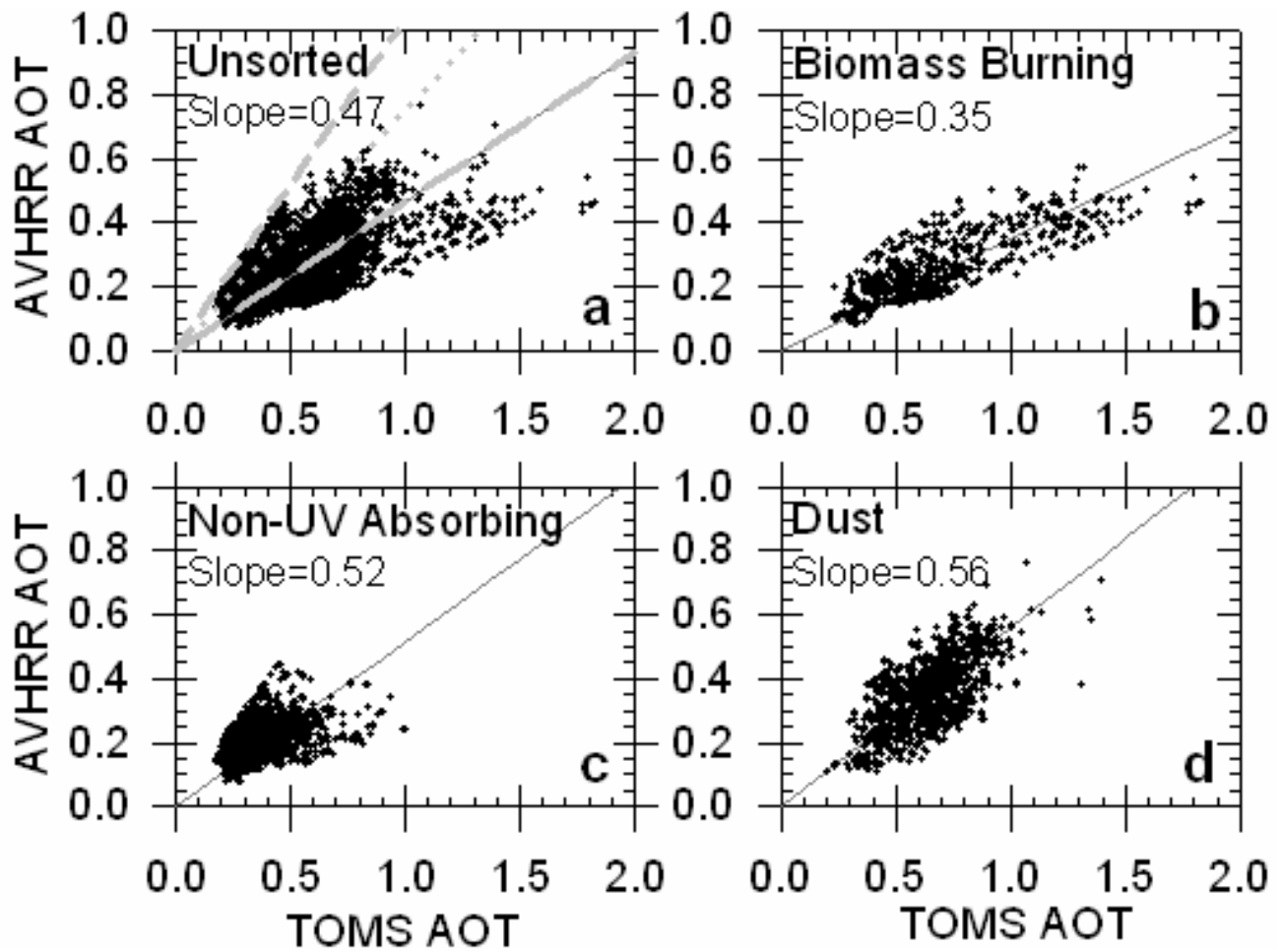


Figure 3. Scatter plots of TOMS AOT as a function of AVHRR AOT for various dominant types of aerosols. Their linear regression lines are marked in panels b-d. In panel a, modeled relationships are given for three dominant aerosol types as used in the TOMS aerosol algorithm: dust (medium-dash line), sulfate (short-dash line), and carbonaceous (long-dash line).

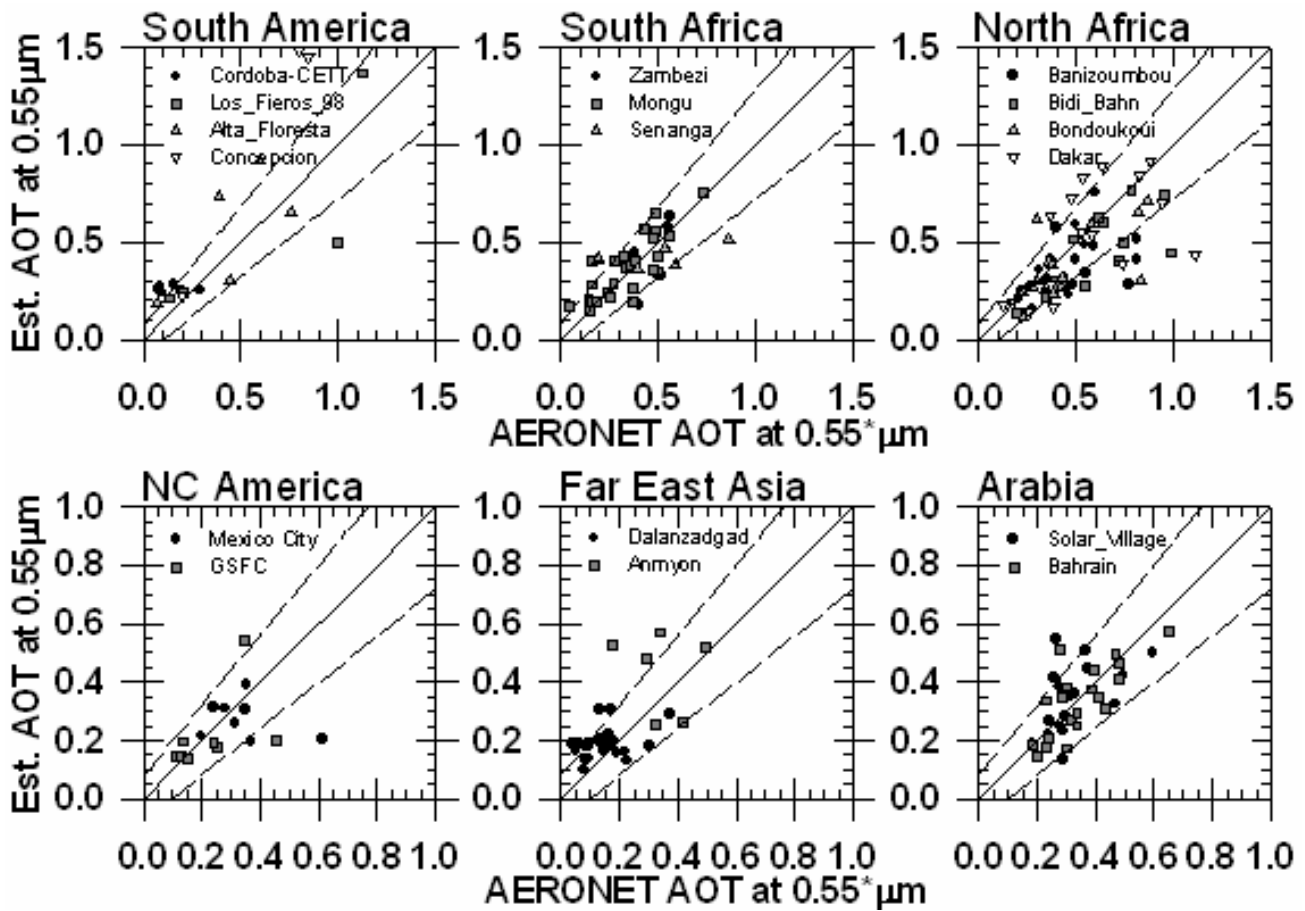


Figure 4. Comparison of estimated AOT over land against monthly AERONET AOT at 0.55 μm. AERONET AOT was interpolated using the Ångström exponent. The solid line is the one-to-one line and dashed lines represent the estimated error range.

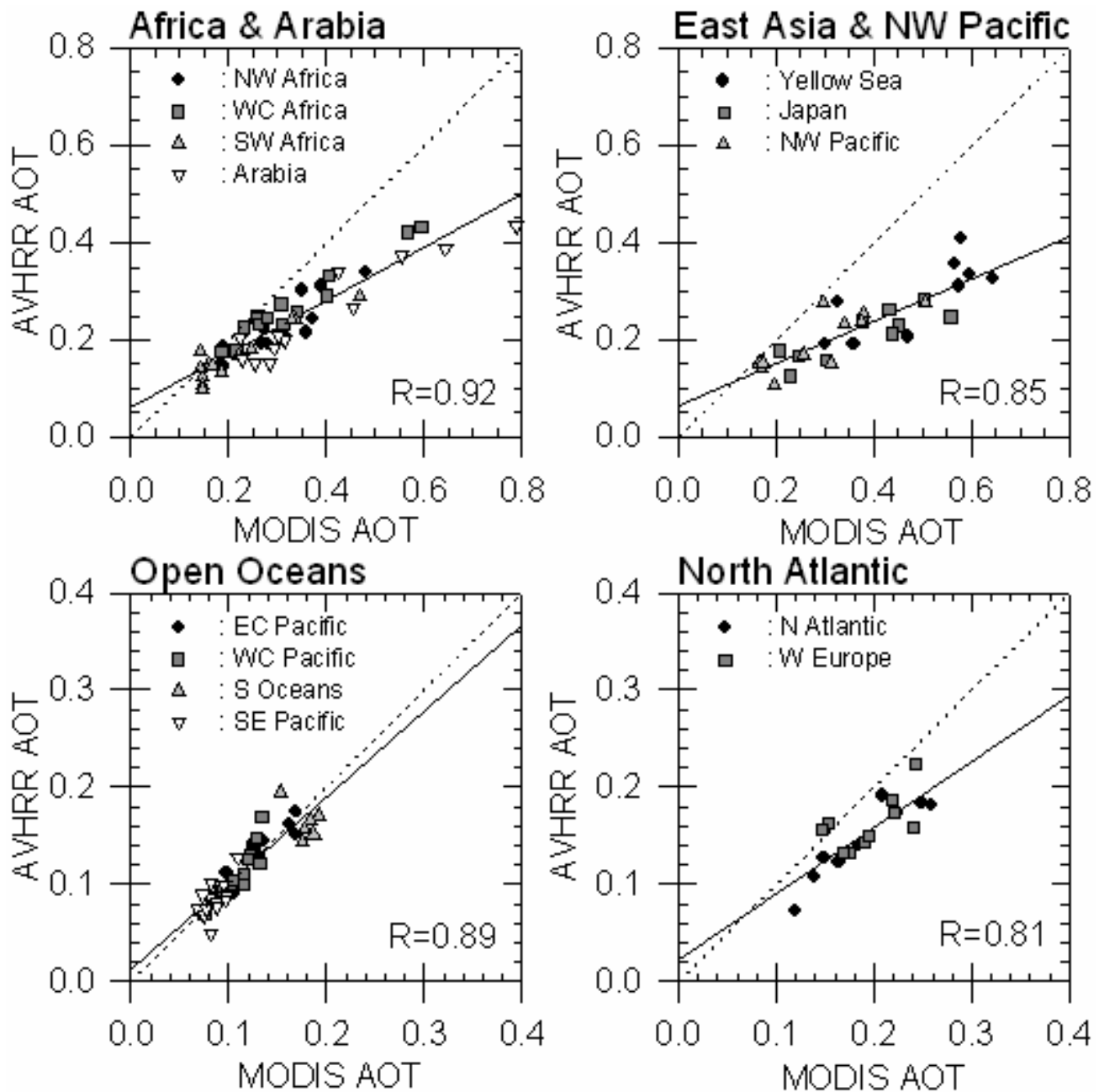


Figure 5. Comparison of co-located AVHRR and MODIS AOTs averaged over each region. Each symbol stands for areal average over some aerosol regimes for individual month. Black solid and dotted lines stand for linear fit curve and one-to-one line, respectively. Note some regions are named referring to the nearby continental locations, but they are all over oceans.

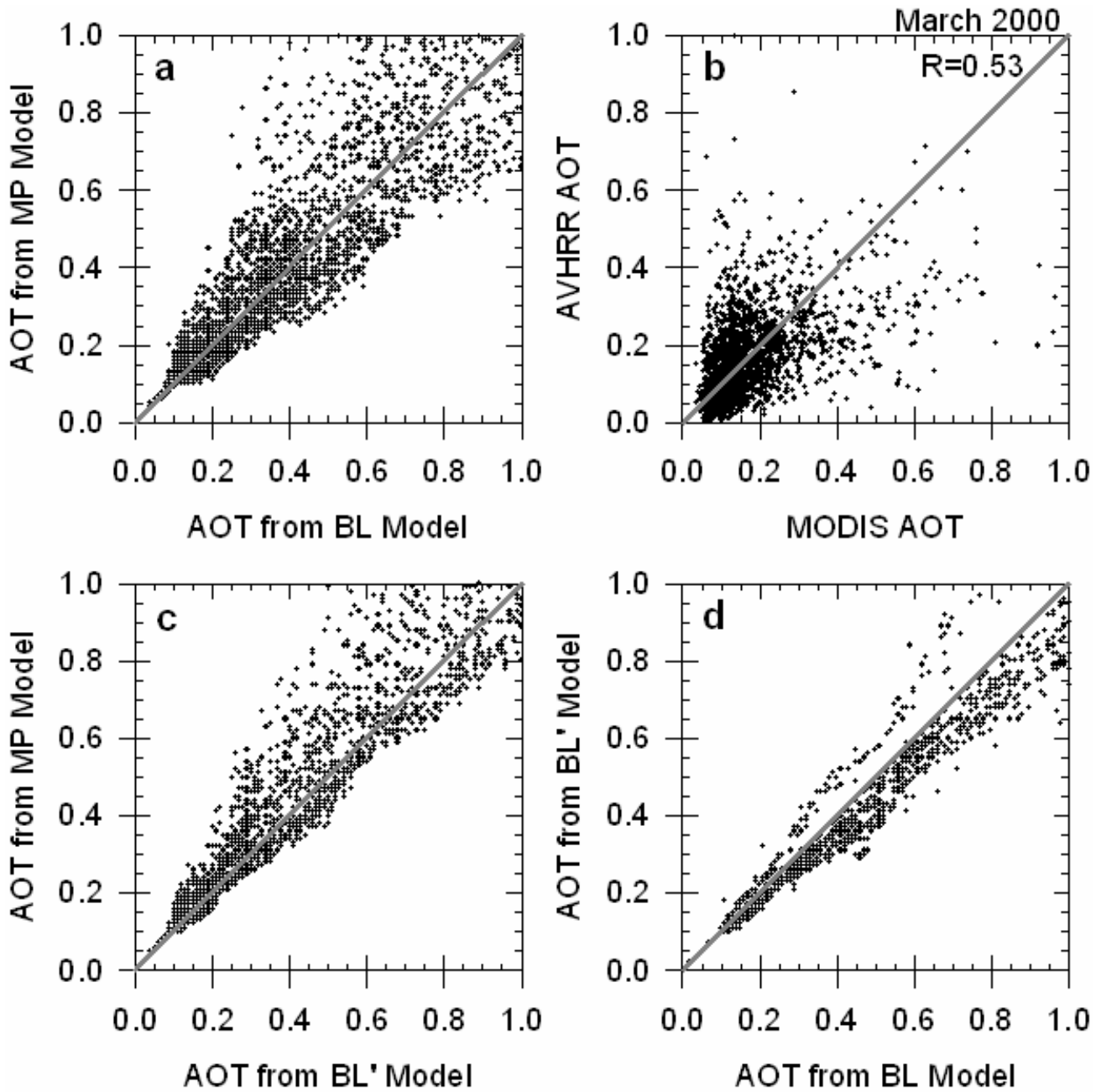


Figure 6. (a) Scatter plot of AOT from MP models versus that from BL models. (b) Scatter plot of observed AOT from MODIS and AVHRR (global, March 2000) (c) The same as Figure 6a but refractive index for BL models were replaced by a single fixed value (i.e., $m=1.5-0.003i$) as used in the MP models, which are referred to as BL' models. (d) Analogous to Fig. 6a and Fig. 6c except for BL' versus BL models. Gray solid line is one-to-one line.

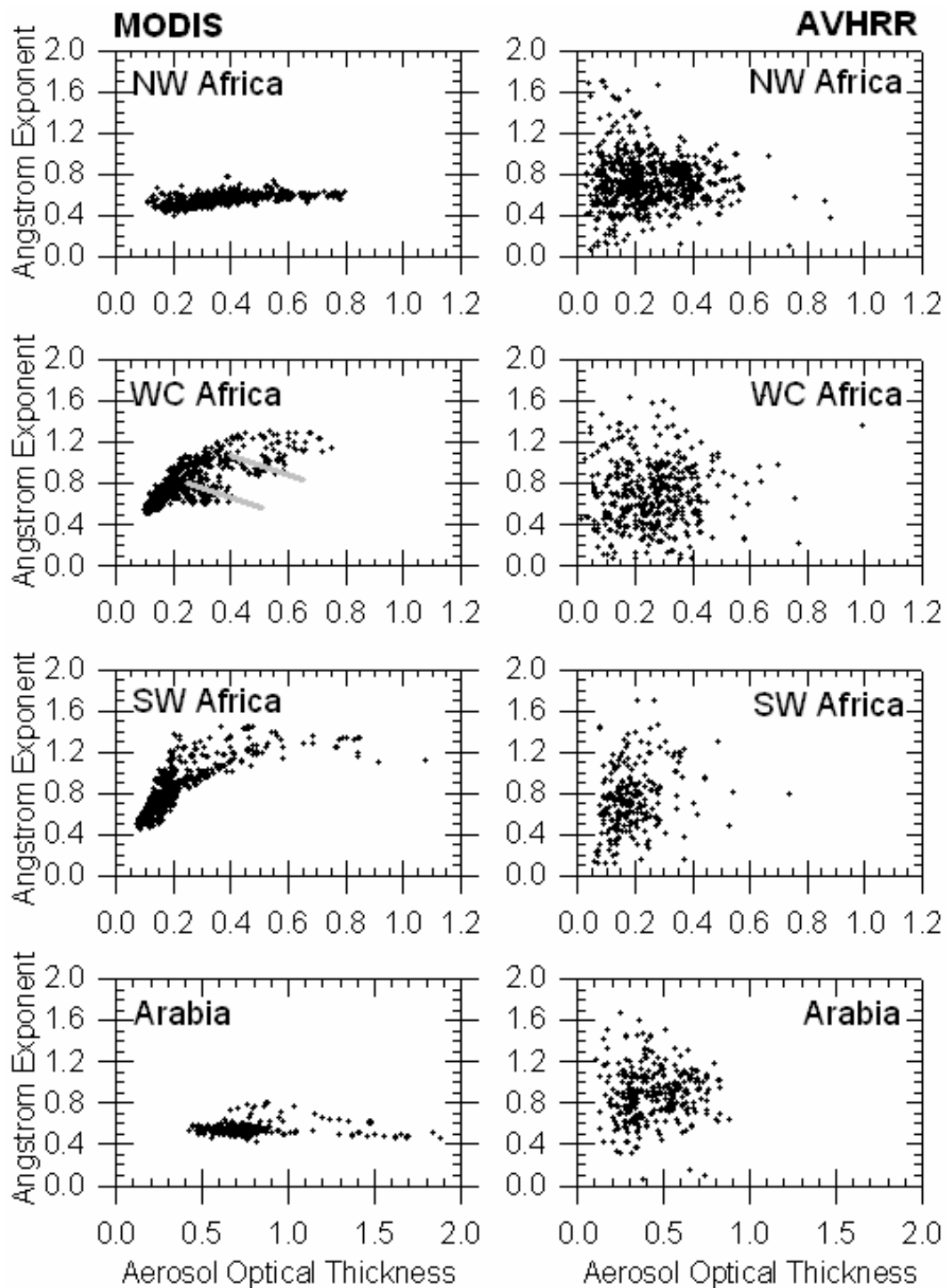


Figure 7. Scatter plots of Ångström exponent versus AOT. Left panels are based on MODIS data while the right panels are from AVHRR data for the same period (July, 2000). Gray lines provided in the WC Africa region for MODIS indicate possible signals from dusts co-existing with biomass burning aerosols in this region.

Acknowledgments

The datasets under study include aerosol optical thickness (AOT) and Angstrom exponent (hereinafter referred to as AVHRR aerosol products) derived from AVHRR under the Global Aerosol Climatology Project (GACP; <http://gacp.giss.nasa.gov/>) by Mishchenko et al. (1999) and Geogdzhayev et al. (2002), and AOT (Torres et al., 1998, 2002) and Aerosol Index (AI) (Herman et al. 1997) from TOMS (<http://toms.gsfc.nasa.gov>). AERONET (<http://aeronet.gsfc.nasa.gov/>) (Holben et al. 1998, 2001) Level 2.0 data and monthly MODIS aerosol products (March 2000~ April 2001, version 4) (Tanré et al. 1997) were also used for the comparison of AVHRR aerosol product. We thank them for providing AVHRR, TOMS, AERONET and MODIS data and guidance for the use of the datasets.

Corresponding Author

M. J. Myeong-Jae Jeong, mjeong@atmos.umd.edu

References

- Geogdzhayev, I. V., M. I. Mishchenko, W. B. Rossow, B. Cairns, and A. A. Lacis, 2002: Global two-channel AVHRR retrievals of aerosol properties over the ocean for the period of NOAA-9 observations and preliminary retrievals using NOAA-7 and NOAA-11 data. *J. Atmos. Sci.*, **59**(3), 262-278.
- Herman, J. R., P. K. Bhartia, O. Torres, C. Hsu, C. Seftor, and E. Celarier, 1997: Global distribution of UV-absorbing aerosols from Nimbus 7/TOMS data. *J. Geophys. Res.*, **102**(D14), 16911-16922.
- Holben, B. N., T. F. Eck, I. Slutsker, D. Tanré, J. B. Buis, A. Setzer, E. Vermote, J. A. Reagan, Y. J. Kaufman, T. Nakajima, F. Lavenue, I. Jankowiak, and A. Smirnov, 1998: AERONET – a federated instrument network and data archive for aerosol characterization. *Remote Sens. Environ.*, **66**, 1-16.
- Holben, B. N., D. Tanré, A. Smirnov, T. F. Eck, I. Slutsker, N. Abuhassan, W. W. Newcomb, J. S. Schafer, B. Chatenet, F. Lavenue, Y. J. Kaufman, J. Vande Castle, A. Setzer, B. Markham, D. Clark, R. Frouin, R. Halthore, A. Kareli, N. T. O'Neill, C. Pietras, R. T. Pinker, K. Voss, and G. Zibordi, 2001: An emerging ground-based aerosol climatology: Aerosol optical depth from AERONET. *J. Geophys. Res.*, **106**(D11), 12067-12097.
- Mishchenko, M. I., I. V. Geogdzhayev, B. Cairns, W. B. Rossow, and A. A. Lacis, 1999: Aerosol retrievals over the ocean by use of channels 1 and 2 AVHRR data: sensitivity analysis and preliminary results. *Appl. Optics*, **38**, 7325-7341.
- Myhre, G. F. Stordal, M. Johnsrud, A. Ignatov, M. I. Mishchenko, I. V. Geogdzhayev, D. Tanré, J.-L. Deuzé, P. Goloub, T. Nakajima, A. Higurashi, O. Torres, B. N. Holben, 2004: Intercomparison of satellite retrieved aerosol optical depth over ocean. *J. Atmos. Sci.*, **61**, 499-513.
- Tanré, D., Y. J. Kaufman, M. Herman, and S. Mattoo, 1997: Remote sensing of aerosol properties over oceans using the MODIS/EOS spectral radiances. *J. Geophys. Res.*, **102**(D14), 16971-16988.

Torres, O., P. K. Bhartia, J. R. Herman, Z. Ahmad, and J. Gleason, 1998: Derivation of aerosol properties from satellite measurements of backscattered ultraviolet radiation: Theoretical basis. *J. Geophys. Res.*, **103**(D14), 17099-17110.

Torres, O., P. K. Bhartia, J. R. Herman, A. Sinyuk, P. Ginoux, and B. Holben, 2002: A long-term record of aerosol optical depth from TOMS observations and comparison to AERONET measurements. *J. Atmos. Sci.*, **59**, 398-413.